Sugarcane Bagasse-derived Hydrochar: Modification with Cations to Enhance Phosphate Removal

Usarat Thawornchaisit*, Tanrawee Onlamai, Nontakorn Phurkphong, and Rawiwan Sukharom

Faculty of Science, King Mongkut's Institute of Technology Ladkrabang, Bangkok 10520, Thailand

ARTICLE INFO

Received: 6 Mar 2021
Received in revised: 26 May 2021
Accepted: 8 Jun 2021
Published online: 15 Jul 2021
DOI: 10.32526/ennrj/19/202100036

Keywords:
Sugarcane bagasse/ Hydrothermal carbonization/ Engineered hydrochar/ Phosphate recovery

*** Corresponding author:**
E-mail: usarat.th@kmitl.ac.th

ABSTRACT

Cation modified hydrochars were synthesized by hydrothermal carbonization (HTC) of sugarcane bagasse, followed by impregnation of three different cations (Ca, Mg, and Fe) or co-precipitation of Fe^{3+} and Fe^{2+}. HTC enhanced the hydrochar surface area and increased the enrichment of oxygen functional groups on the hydrochar surface confirmed by FTIR. The oxygen functional groups further improve the adsorption capacity for cations during hydrochar chemical modification. Physical appearance, FTIR and XRF confirmed that Ca^{2+}, Mg^{2+} and Fe^{2+} or Fe^{3+} were well retained in the bagasse-derived hydrochar. The pH_{pzc} values of all chemically modified hydrochars were greater than the unmodified hydrochar or bagasse alone. Modification with different cations improved phosphate uptake capacity. The Fe-modified hydrochar with about 45-50% Fe content showed greater phosphate removal efficiency than Ca- and Mg-modified hydrochars. In addition, hydrochars decorated by impregnation of Fe^{3+} demonstrated better phosphate removal than ones produced by co-precipitation of Fe^{3+} and Fe^{2+}. Thus, chemically modified hydrochars could be used as an environmentally alternative adsorbent for phosphate removal from aqueous solutions.

1. INTRODUCTION

Sugarcane bagasse (SB), the solid fibrous material remaining from sugarcane juice extraction, is the main residue from the sugar industry. Approximately 270-280 tons of bagasse are generated from every 1,000 tons of processed sugarcane (Martinez-Hernandez et al., 2018). The world generated about 1,900 megatons of bagasse (mostly in Latin America and Asia) in the past five years (Mokhena et al., 2018). Bagasse availability is expected to increase, due to the increasing demand for sugar in households as well as industrial use. The bagasse is currently used as a biofuel within the sugar industry itself, and in biomass power plants for steam generation and electricity with a challenging operation issue related to its high moisture content, which is typically 40-50 percent (Congsomjit and Areeprasert, 2020). Considering 80-85% of sugarcane bagasse is used for energy generation within the plant, and about 15 to 20 percent of bagasse is left unused at some factories after energy needs are met (USDA, 2018), bagasse is an ideal raw material that needs to increase its added value.

Synthesis of hydrochar via hydrothermal carbonization (HTC) has been investigated as an approach for increasing biomass valued-products. Conversion of biomass waste to adsorbent for removal of organic and inorganic contaminants is an environmental aspect that has received considerable attention due to its simplicity and ability to produce hydrochars with attractive characteristics that promote effective use in dealing with pollutant contamination in aqueous solution (Jain et al., 2016; Nguyen et al., 2019). HTC is the thermochemical conversion technique in a closed reactor that uses moderate processing temperature (180-240°C) and water as carbonatization medium under self-generated pressures to react with wet/dry materials and convert the biomass into solid materials, namely hydrochar (Congsomjit and Areeprasert, 2020; Dai et al., 2014). HTC process offers significant advantages over pyrolysis, a conventional utilized process for biomass-to-carbon-based products conversion, in terms of mild reaction condition, lower energy consumption process, and the ability to deliver hydrochar with high concentrations of oxygenated

Citation: Thawornchaisit U, Onlamai T, Phurkphong N, Sukharom R. Sugarcane bagasse-derived hydrochar: Modification with cations to enhance phosphate removal. Environ. Nat. Resour. J. 2021;19(5):371-380. (https://doi.org/10.32526/ennrj/19/202100036)

functional groups (OFGs, i.e., carboxylic, hydroxyl, and phenolic) on the surface (Jain et al., 2016; Nguyen et al., 2019; Petrović et al., 2016). The relative abundance of OFGs on hydrochar's surface plays an important role in the adsorption capacity of hydrochar toward the given contaminants. Higher OFGs on the adsorbents resulted in higher adsorption capacity for the contaminants, especially positively charged contaminants, in an aqueous solution (Almarri et al., 2009; Hotová et al., 2020). This characteristic is a major reason for higher uptake capacity of hydrochar than biochar toward polar and nonpolar contaminants, including bisphenol-A, 17α-ethinyl estradiol, and phenanthrene (Sun et al., 2011), as well as methylene blue, iodine and copper ions (Jian et al., 2018). Although hydrochar showed a great potential adsorbent for cationic contaminants, the adsorption capacity for anions (i.e., phosphate, nitrate, arsenate) is very limited due to a large amount of OFGs, making the hydrochar's surface more negatively charged, subsequently repelling negatively charged compounds (Fang et al., 2015; He et al., 2019).

Phosphorus is an essential nutrient for the growth, functioning and reproduction of all life on earth, and is a non-renewable resource to produce phosphorus (P) based chemicals, mainly as mineral fertilizers (Tarayre et al., 2016). Phosphorus is naturally found in geological deposits of phosphate rock, which are found mostly in Morocco and Western Sahara (Cordell and White, 2013; Desmidt et al., 2015; USGS, 2021). In recent years, the depletion of phosphate rock natural reserves and phosphorus future availability has received great attention, thus phosphorus has been listed as one of the critical raw materials for the European Union since 2014 (European Commission, 2020). Apart from mineral reserves (i.e. phosphate rock), phosphorus has been found in natural water bodies (freshwater lakes, reservoirs and rivers). Phosphorus flow to an aquatic ecosystem is from soil erosion, agricultural runoff, and point source discharges. Discharge of municipal wastewaters and the effluent discharged from wastewater treatment plants (WWTPs) is an important point source of phosphorus loading (Kundu et al., 2015; Qin et al., 2015). Low concentrations of phosphorus benefit the biological productivity of the aquatic ecosystem, however excessive phosphorus inputs can cause eutrophication, a worldwide water quality deterioration. The phenomenon often leads to the reduction in oxygen concentrations, which affects not only benthic invertebrates but also the spawning success rate of some important fish species (Murray et al., 2019). To address the dual problems of phosphorus future availability and P-based eutrophication, technologies for removal and recovery of phosphorus from wastewater and its possible reuse is necessary and a long-term sustainable solution (Carrillo et al., 2020).

Application of natural agricultural residue for P-adsorption have been investigated, however the adsorption capacity of most natural materials is usually less than 1 mgP/g (Carrillo et al., 2020). Interest in agricultural hydrochars that are rich in oxygen-containing functional groups as adsorbents in water and wastewater treatment has increased. However, their ability for phosphate removal is quite low. To further enhance the phosphate sorption ability of hydrochar, several studies have investigated different methods of tailoring the hydrochar's surface structure. Deposition of mineral oxides and salts is one of the chemical modification methods that is widely applied to change the surface electrical properties of hydrochar (Azzaz et al., 2020). Research has shown that decorating hydrochar surface through impregnating or coating cationic minerals such as Fe, Mg, Ca, La, Al, Mg/Al, either before or after HTC, could develop effective adsorbents with improved adsorption capacity for anionic pollutants (Dai et al., 2014; He et al., 2019; Yu et al., 2019). However, the information about the effects of modifying cationic minerals on the phosphate removal capability of hydrochar is limited. In addition, growing concerns about phosphorus (P) future availability (Alewell et al., 2020; European Commission, 2017) as well as its detrimental environmental impacts like eutrophication, have made the recycling of P crucial to sustainable development (Cordell and White, 2013). Along with the presence of sugarcane bagasse as a common agricultural and industrial waste, this study demonstrates the utilization of hydrothermal carbonization as an approach for adding value to sugarcane bagasse. In addition, this study investigates the effects of different types of modifying agents on the efficiency and selectivity of sugarcane bagasse-modified hydrochar for phosphate adsorption.

2. METHODOLOGY

2.1 Materials and chemicals

Sugarcane bagasse was acquired from a roadside juice hawker in Bangkok, Thailand. After washing several times with tap water and deionized water (DI-water) to remove any adhering dirt, it was dried at 60°C for 24 h and cut into small pieces (about

25 mm length). The bagasse was ground, passed through a 70-mesh sieve, and then stored in a sealed container until use. All chemical reagents used in this study were analytical grade.

2.2 Preparation and modification of hydrochars

Hydrothermal carbonization of bagasse conducted in a 1 L Parr stirred pressure reactor with a 4848-reactor controller, following Hoekman et al. (2011). In a typical synthesis, 70 g of prepared bagasse was mixed with DI-water-1:8 bagasse/water ratio (w/v). The reactor and contents were then heated, while stirring, until the reaction temperature was at 230ºC and held for 1 h reaction time. At the end of the holding time, the vessel was cooled to 45ºC. The solid and aqueous products were separated by vacuum filtration, the hydrochars (HC) were then washed with DI-water, followed by oven drying at 105ºC for 24 h.

The hydochars were modified with Ca, Mg, and Fe, following Yang et al. (2018). To prepare the modified hydrochars, the solutions of calcium chloride ($CaCl_2$), magnesium chloride ($MgCl_2$), ferric chloride hexahydrate ($FeCl_3 \cdot 6H_2O$), and a mixture of ferric chloride hexahydrate ($FeCl_3 \cdot 6H_2O$) and ferrous sulfate heptahydrate ($FeSO_4 \cdot 7H_2O$) were prepared by dissolving a predetermined amount of each compound in DI-water. Subsequently, a measured amount of hydrochar was immersed in one of the solutions and stirred at 150 rpm for 10 min, followed by dropwise addition of 1 M NaOH until the pH was at 11. The suspension was continuously stirred for 45 min and aged without stirring for 24 h at room temperature. Then, the acquired mixtures were washed with deionized water to remove residual salts and loosely attached minerals until the pH of the washing solution equals the of the DI water (pH 6.0-6.5), followed by drying (105ºC, 24 h). The final products were labeled as Ca-HC, Mg-HC, Fe(III)-HC, and Fe(III)/Fe(II)-HC.

2.3 Characterization of sugarcane bagasse and hydrochars

The surface morphology of the bagasse and the hydrochars was characterized by a scanning electron microscope (SEM, QUANTA FEG-250, FEI, USA). C, H, and N compositions were determined by an elemental analyzer (LECO 628 series, LECO Corporation, USA). Methylene blue adsorption studies, following Nunes and Guerreiro (2011), were used to estimate the surface areas of biomass and hydrochars. A Fourier transform infrared spectrometer (FTIR, Spectrum GX, Perkin Elmer) within 400-4,000 cm^{-1} range, was used to identify surface functional groups. An X-ray Fluorescence Spectrometer (XRF, SRS3400, Bruker, Germany) was used to determine the composition of inorganics in hydrochar and the modified hydrochars. The pH at the point of zero charges (pH_{pzc}) was determined by using the pH drift method of 0.01 M NaCl with a pH interval of 1 and in the range of between 3 and 11 (Thawornchaisit et al., 2019).

2.4 Phosphate removal experiments

A stock phosphate solution was prepared by dissolving KH_2PO_4 in distilled water. The phosphate removal capability from aqueous solutions of bagasse and the hydrochars was measured by mixing a 0.1 g sample with 50 mL phosphate solution (pH 7, 25 mg P/L). The mixtures were mechanically shaken at a constant 150 rpm speed. At defined time intervals, the mixtures were immediately filtered through a 0.45 µm filter, and the concentration of phosphate in the filtrates was measured based on the 4500-PE: Ascorbic Acid Method (APHA et al., 2012).

3. RESULTS AND DISCUSSION

3.1 Physicochemical properties of hydrochars

3.1.1 Morphological and textural properties

Bagasse samples were a pale creamy yellow color (Figure 1(a)). Hydrothermal carbonization at 230ºC for 1 h turned the hydrochar into grayish-black solids (Figure 1(b)), confirming the success of lignocellulosic biomass conversion to carbon-rich materials.

(a) (b)

Figure 1. Images of (a) sugarcane bagasse and (b) the derived hydrochar.

Bagasse SEM images show relatively well-defined surfaces with little flaking observed on the surface (Figure 2(a)). In contrast, the image, labeled (b), of the sugarcane bagasse-dervied hydrochar shows a high degree of surface roughness and numerous microspheres with different shapes and sizes indicating destruction and degradation of the cell wall. The new microspheres on the hydrochar surface were ascribed to the decomposition of hemicellulose, as well as

depolymerization of cellulose and partial degradation of lignin (Cai et al., 2016; Jain et al., 2016).

3.1.2 Elemental composition

CHN elemental analysis showed that hydrochar had significantly higher carbon content than the raw bagasse, as a result of carbonization (Table 1). The C content increased from 45% in sugarcane bagasse to 61% in the hydrochar. On the other hand, a slight reduction in hydrogen content was observed in the hydrochar compared to its content in the sugarcane bagasse. Dehydration and decarboxylation were reported to be the paths that were responsible for the reduction of hydrogen and oxygen contents in hydrochar (Cai et al., 2016). Meanwhile, the nitrogen contents of the hydrochar increase, which were consistent with that reported by Congsomjit and Areeprasert (2020) and the HTC of other kinds of lignocellulosic biomass (Xiao et al., 2012; Cai et al., 2016).

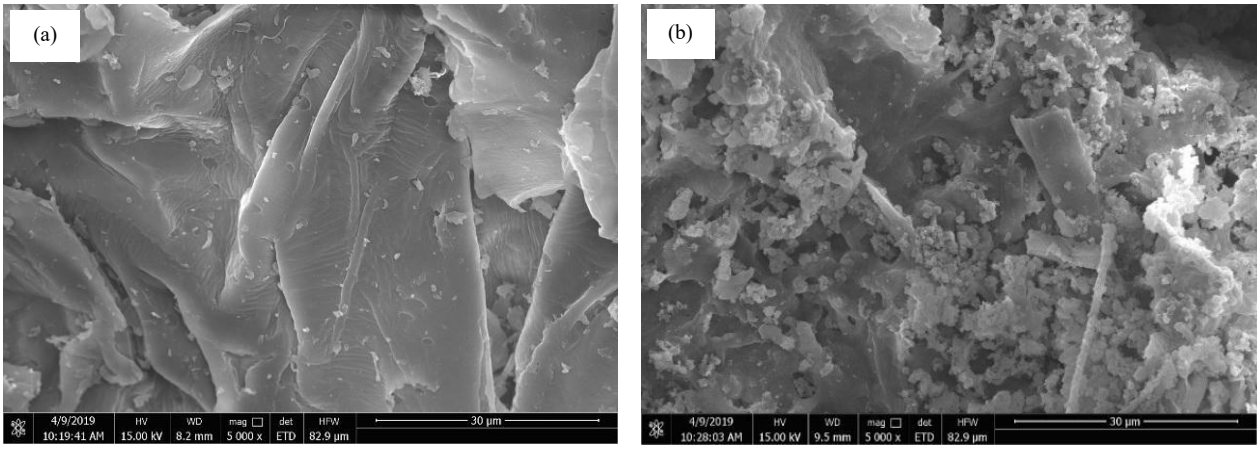

Figure 2. SEM images of sugarcane bagasse (a) and the derived hydrochar (b).

Table 1. Composition of sugarcane bagasse and hydrochars determined by CHN elemental analysis

Sample	Elements (%)		
	C	H	N
SB	45.44	6.29	0.12
HC	60.99	5.64	0.23

3.1.3 Surface functionality

FTIR were recorded to understand chemical changes in the bagasse and the derived hydrochars during HTC. As shown in Figure 3, the IR spectra of the hydrochars were quite similar to that of the raw biomass. The OH-group stretching vibration at 3,346-3,416 cm^{-1}, was ascribed to the hydroxyl group, and the C-H stretching vibration appears at 2,923-2,929 cm^{-1}, indicating a presence of aliphatic structures, identified in both bagasse and hydrochar samples. The 1,733 cm^{-1} band, ascribed to C=O stretching vibrations in the hemicellulose (Wang et al., 2017), disappeared from the hydrochar. In contrast, the 1,112 cm^{-1} band, associated with cellulose (Guo et al., 2015) was sharper in HC when compared to the raw materials. This confirmed hydrolysis of hemicellulose content with hydrothermal carbonization of the bagasse. The 1,510 cm^{-1} peak, attributed to aromatic ring stretching vibration (Guo et al., 2015), was also sharper in the hydrochar. This showed removal of the amorphous fraction in the biomass as suggested by Guo et al. (2015). In contrast, the peak at 1,699 cm^{-1}, corresponding to the carboxyl, carbonyl, or ester groups, was observed only in the hydrochar samples. Wang et al. (2017) noted that the 1,699 cm^{-1} peak indicated the presence of oxygen-containing functional groups, confirming that HTC enhanced oxygen group content and further improved the reactivity of the hydrochar.

3.1.4 Specific surface area

Methylene blue number (MBN) was 40±11 mg/g for bagasse and 101±18 mg/g for the hydrochar. The higher number for the hydrochar showed that HTC increased the biomass surface area. This is consistent with other studies of HTC of lignocellulosic materials (Cai et al., 2016; Niinipuu et al., 2020) and was attributed to the disintegration of the physical structure of biomass, followed by degradation of hemicellulose and cellulose (Jain et al., 2016).

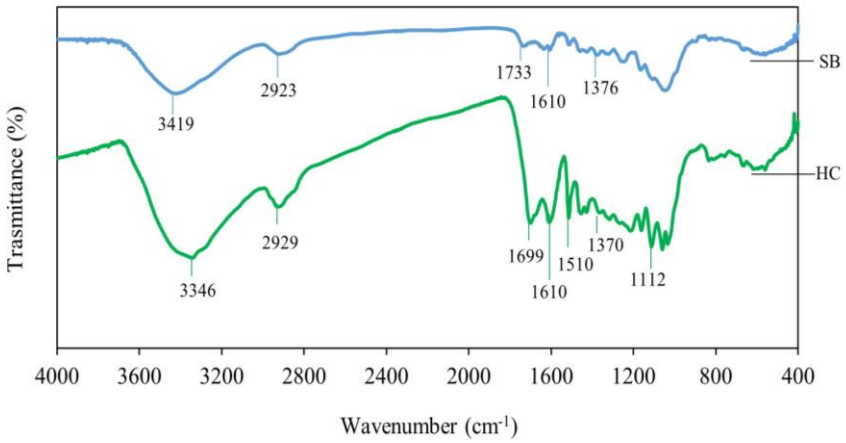

Figure 3. FTIR spectra of sugarcane bagasse (SB) and the derived hydrochar (HC).

3.2 Physicochemical properties of metal modified hydrochars

3.2.1 Physical appearance

Images of modified hydrochar are presented in Figure 4. In the case of Ca-HC and Mg-HC, the material color was completely black compared with the sugarcane-derived hydrochar (Figure 1(b)). On the contrary, when Fe^{3+} and a combination of Fe^{3+} and Fe^{2+} were added to a hydrochar, the products had an orange-red tone, which indicated successful mineral impregnation or coating.

(a) (b) (c) (d)

Figure 4. Images of cation-modified hydrochars (a) Ca^{2+}, (b) Mg^{2+}, (c) Fe^{3+}/ Fe^{2+} and (d) Fe^{3+}.

3.2.2 Elemental composition by XRF

Data obtained from XRF revealed that the major mineral in the hydrochar was silica (Si), with a SiO_2 content of 52.7% (Table 2). Si content in the hydrochar dropped after impregnation or coating with metals. A significant reduction of SiO_2 was attributed to the release of silicon components during NaOH post-treatment of the metal impregnation or co-precipitation process in Equation (1) (Tang et al., 2019).

$$nSiO_2 + 2NaOH \rightarrow Na_2O \cdot nSiO_2 + H_2O \quad (1)$$

Compared to the original hydrochar, compositions of Ca, Mg, and Fe were higher confirming the surface modification of the hydrochar with these cations. In addition, Fe content in both Fe modified hydrochars was relatively greater than Ca or Mg contents. This was related to the metal affinity with the oxygenated functional groups in hydrochar. Fe, especially Fe^{3+}, has a greater ionic charge than Ca^{2+} and Mg^{2+}. Subsequently, interaction between Fe^{3+} and oxygen functional groups of hydrochar would be more favorable.

Table 2. Elemental compositions of hydrochar and modified hydrochars determined by XRF.

Elements	Contents (%)				
	HC	Ca-HC	Mg-HC	Fe(III)/Fe(II)-HC	Fe(III)-HC
SiO_2	52.7	ND	ND	ND	ND
Al_2O_3	9.94	35.0	77.9	18.3	19.3
Fe_2O_3	4.02	ND	ND	54.0	43.8
CaO	1.37	19.9	ND	ND	ND
MgO	5.05	ND	14.93	ND	ND
Na_2O	ND	8.95	2.09	9.87	10.4

Table 2. Elemental compositions of hydrochar and modified hydrochars determined by XRF (cont.).

Elements	Contents (%)				
	HC	Ca-HC	Mg-HC	Fe(III)/Fe(II)-HC	Fe(III)-HC
K_2O	3.38	4.15	3.46	3.89	2.88
CoO	ND	ND	1.02	ND	ND
CuO	2.54	ND	0.460	0.406	0.291
ZnO	ND	ND	ND	ND	0.175
P_2O_5	5.52	ND	ND	ND	ND
Cl	3.99	17.8	ND	4.73	7.79
SO_3	12.3	5.90	ND	9.03	7.54

3.2.3 Surface functionality

To understand chemical changes in hydrochars after surface modification with different cations, FTIR spectra were recorded for the original hydrochar and cation-impregnated hydrochars. As shown in Figure 5, the 1,699 cm^{-1} band, ascribed to the carboxyl, carbonyl, or ester groups on the hydrochar surface, was noticeably weakened, especially in Ca-, and Fe-hydrochars. The band at 757 cm^{-1} became stronger in the Ca-HC, confirming the interaction of the cation with the oxygenated functional groups on hydrochar. On the contrary, the characteristic peaks of Mg-HC were similar to those of the unmodified hydrochar. Fang et al. (2014) also observed this when corn-derived biochar was impregnated with $MgCl_2$, and their explanation was given that the magnesium nanoparticles did not affect the structural formation of organic functional groups in Mg-modified biochar. For Fe-modified hydrochars, Fe incorporation was confirmed by bands at 550 cm^{-1} and 460 cm^{-1}, representing hematite (Mahmoud, 2017). These two bands were found in all hydrochars decorated by Fe^{3+} (Fe(III)-HC) or a combination of Fe^{3+} and Fe^{2+}(Fe(III)/Fe(II)-HC). A peak of Fe-O at 580 cm^{-1} was also found in Fe(III)/Fe(II)-HC. This was also reported in Yang et al. (2018), confirming that Fe^{3+}/Fe^{2+} had been coated on the hydrochars.

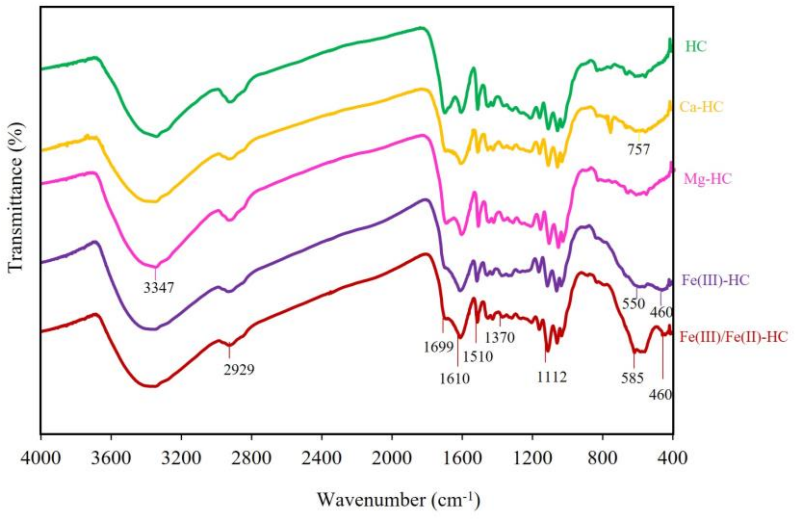

Figure 5. FTIR spectra of hydrochar (HC) and Mg^{2+}-modified hydrochar (Mg-HC), Ca^{2+}-modified hydrochar (Ca-HC), Fe^{3+}/Fe^{2+} modified hydrochar (Fe(III)/Fe(II)-HC) and Fe^{3+} modified hydrochar (Fe(III)-HC).

3.2.4 pH_{pzc}

Points of zero charge (pH_{pzc}) were determined for bagasse and the modified hydrochars using the pH drift method, measuring pH where the material behaves as a neutral species. The values of pH differences (final pH-initial pH, ΔpH) were plotted versus their corresponding initial pH (pH_i)-see Figure 6. From the graphs, pH_{pzc} of the materials were determined from the point of intersection on the x-axis in Figure 6.

Figure 6 shows that bagasse and its derived hydrochars had acidic surfaces, with pH_{pzc} approximately 4. Thus, binding of cations was favored for $pH>pH_{pzc}$, due to deprotonation of the surface

functional groups, resulting in a negatively charged surface which attracts cations. After cations were added by either impregnation or co-precipitation, the surfaces were less acidic, as seen from the shift of pH_{pzc} to the higher value (Figure 6). The pH_{pzc} of Ca-HC and Mg-HC were similar at approximately 7, while the points of zero charge (pzc) were at pH 5.6 for Fe(III)/Fe(II)-HC and pH 8.0 for Fe(III)-HC. The presence of sulfate in the materials used to synthesize Fe(III)/Fe(II)-HC could be the reason for shifting the Fe(III)/Fe(II)-HC pH_{pzc} to lower pH as reported by Kosmulski (2016). The higher pH_{pzc} of the metal-modified hydrochars compared to bagasse and the original hydrochar indicated that phosphate removal was feasible below this pH, because the net positively charged surfaces was favorable and facilitated the removal of anions.

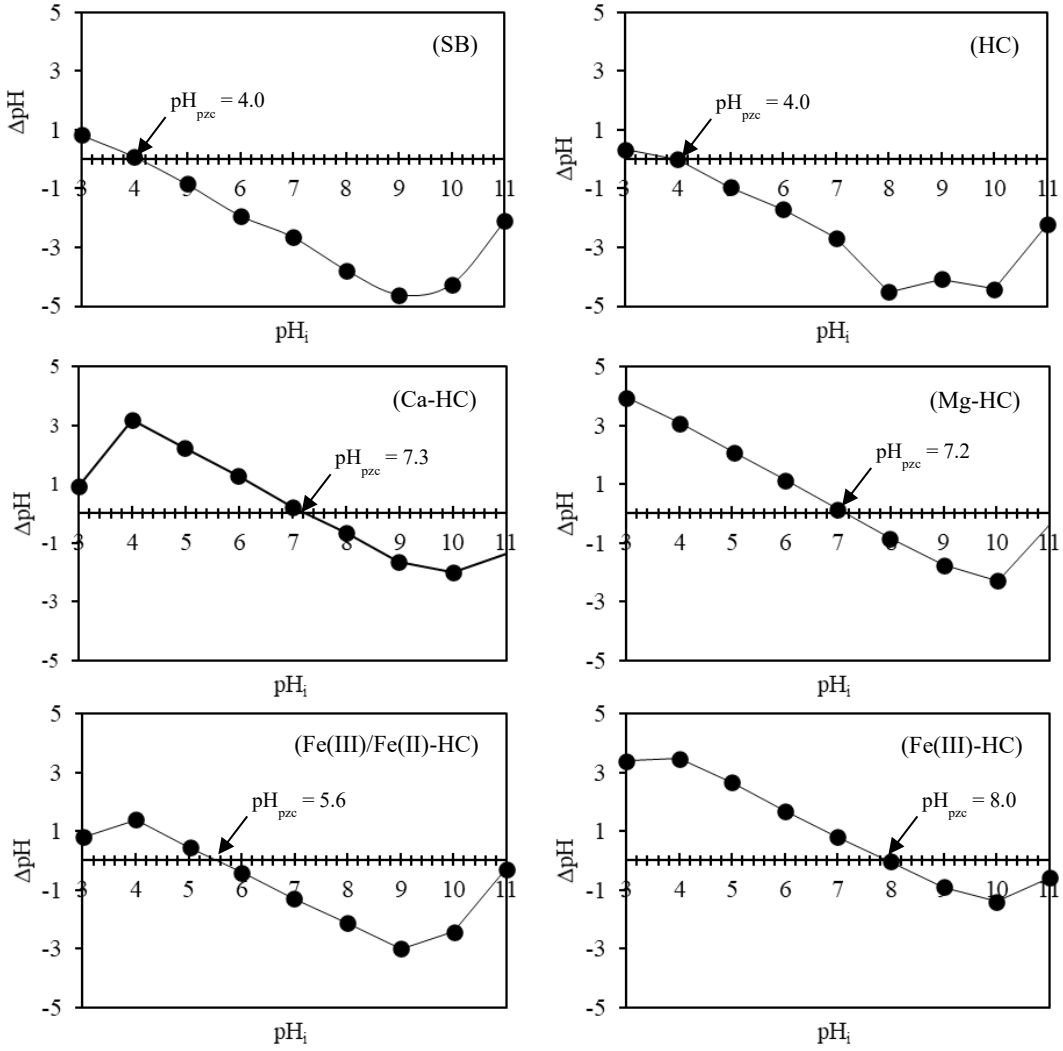

Figure 6. Plot to determine pH_{pzc}: SB=sugarcane bagasse, HC=unaltered and modified hydrochars, Ca-HC=Ca^{2+}, Mg-HC=Mg^{2+}, Fe(III)/Fe(II)-HC=Fe^{3+}/Fe^{2+}, and Fe(III)-HC=Fe^{3+}.

3.3 Phosphate removal capacity

Figure 7 shows the phosphate removal efficiency of the hydrochars. It can be seen that hydrothermal carbonization followed by chemical impregnation or coating transforms sugarcane bagasse into an effective phosphate adsorbent. Phosphate was removed more effective by the hydrochar than the raw material (Figure 8). The surface roughness and numerous microspheres on the hydrochar surface facilitated physisorption of phosphorus from aqueous solution.

The modifying cations enhanced phosphate removal: phosphate removal efficiencies were greater than the unmodified hydrochar (Figure 7 and 8). Phosphate removal was efficient when Fe-modified hydrochars, especially Fe^{3+}-modified hydrochar, were used, yielding the highest adsorption capacity (Figure 8). Moreover, hydrochar decorated with Fe^{3+} in

alkaline conditions showed higher phosphate removal than hydrochars decorated with co-precipitation of Fe^{3+}/Fe^{2+}. A similar observation was reported when rice straw biochar was decorated by impregnation of Fe^{3+} compared to biochar decorated by co-precipitation of Fe^{3+}/Fe^{2+} (Thawornchaisit et al., 2019). The high phosphate removal by Fe(III)-HC was attributed to the presence of $Fe(OH)_3$ and Fe_2O_3 that existed in the Fe^{3+}-modified hydrochar (Yang et al., 2018). In addition, the difference in phosphate removal capacity between the Fe(III)-HC and Fe(III)/Fe(II)-HC could be related to the pHpzc values. pHpzc values were 5.6 for Fe(III)/Fe(II)-HC and 8.0 for Fe(III)-HC. The charge on the Fe(III)-HC surface was more positive, since phosphates removal experiments were conducted at pH<pHpzc, then the phosphate interaction occurred more favorably for Fe(III)-HC.

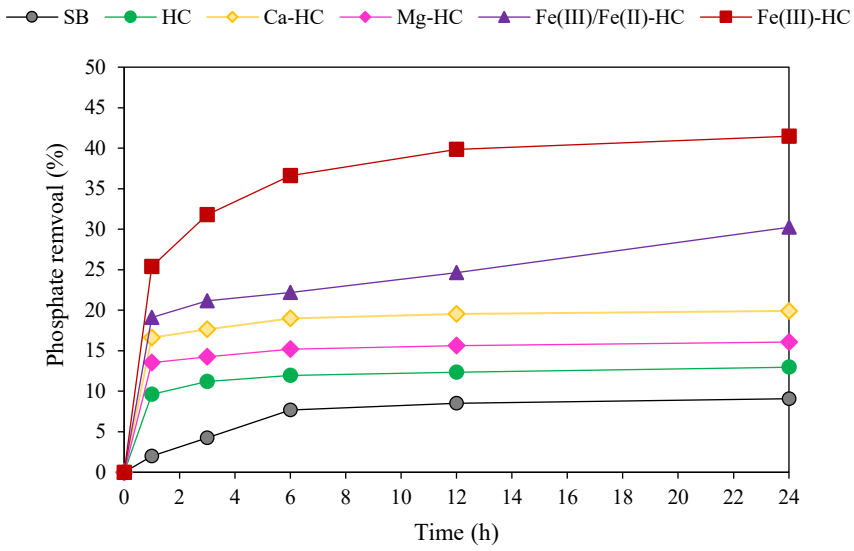

Figure 7. Effect of different modifying cations on phosphate removal ability of sugarcane bagasse (SB), hydrochar (HC), and cation-modified hydrochars.

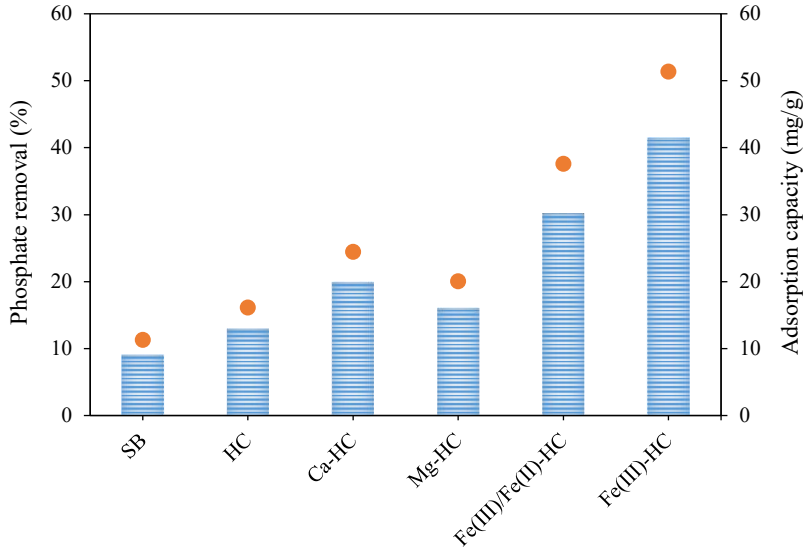

Figure 8. Phosphate removal ability (bar) and phosphate adsorption capacity (orange dot) of cation-modified hydrochars in contact with a 25 mg P/L of KH_2PO_4 solution for 24 hours.

In the Mg- and Ca-modified hydrochars, phosphate removal was observed but less than Fe-modified hydrochars. This phenomenon was attributed to the different valence states: Fe^{3+} with a higher charge density and considered to be a hard acid, would have a greater affinity for a hard base, like PO_4^{3-}, than Ca^{2+} or Mg^{2+}. Therefore, reaction between PO_4^{3-} and Fe^{3+} would be more favorable through a combination

of electrostatic attraction, surface complex formation and anion exchange as reported by Yang et al. (2018). In addition, the amount of Fe in the hydrochar also played an important role in phosphate removal. XRF analysis (see Table 2) revealed that Fe modified hydrochar had higher Fe concentration than Ca- and Mg-modified biochar, thus it removed phosphate more efficiently.

4. CONCLUSION

Hydrothermal carbonization (HTC), followed with impregnating or coating with cations including Ca, Mg or Fe was applied to sugarcane bagasse for producing a solid char product, or hydrochar, with improving phosphate removal capability. Bagasse surfaces became much rougher with more fragmentation than the starting materials after HTC. Higher methylene blue number in hydrochars compared with bagasse showed an increased surface area for adsorption of contaminants. HTC also improved reactivity through the formation of oxygenated functional groups on the hydrochar, which made it an effective precursor for the production of cation-modified hydrochars. Phosphate removal was improved when hydrochars were decorated with Ca^{2+}, Mg^{2+}, Fe^{3+}, and Fe^{3+}+Fe^{2+} under alkaline conditions. Fe-rich hydrochars demonstrated better phosphate removal capacity. We concluded that impregnation or coating on the hydrochar surface after HTC was able to produce effective functional adsorbent for anionic pollutants, like phosphates.

ACKNOWLEDGEMENTS

The authors would like to thank the Department of Chemistry, Faculty of Science, KMITL for financial support for a student's Special Project of TO, NP and RS. Special thanks to John Morris, the author of "Keep it Simple: a guide to English Technical writing" and a member of the Research Clinic, KMITL Research and Innovation Services (KRIS) for shortening and removing unnecessary color from the paper.

REFERENCES

Alewell C, Ringeval B, Ballabio C, Robin son DA, Panagos P, Borrelli P. Global phosphorus shortage will be aggravated by soil erosion. Nature Communications 2020;11:4546.

Almarri M, Ma X, Song C. Role of surface oxygen-containing functional groups in liquid-phase adsorption of nitrogen compounds on carbon-based adsorbents. Energy and Fuels 2009;23(8):3940-7.

American Public Health Association (APHA), American Water Works Association (AWWA), and Water Environment Federation (WEF). Standard Methods for the Examination of Water and Wastewater. 22nd ed. Washington, D.C., USA: APHA-AWWA-WEF; 2012. p. 153-5.

Azzaz AA, Khiari B, Jellali S, Ghimbeu CM, Jeguirim M. Hydrochars production, characterization and application for wastewater treatment: A review. Renewable and Sustainable Energy Reviews 2020;127:109882.

Cai J, Li B, Chen C, Wang J, Zhao M, Zhang K. Hydrothermal carbonization of tobacco stalk for fuel application. Bioresource Technology 2016;220:305-11.

Carrillo V, Fuentes B, Gomez G, Vidal G. Characterization and recovery of phosphorus from wastewater by combined technologies. Reviews in Environmental Science and Biotechnology 2020;19:389-418.

Congsomjit D, Areeprasert C. Hydrochar-derived activated carbon from sugar cane bagasse employing hydrothermal carbonization and steam activation for syrup decolorization. Biomass Conversion and Biorefinery 2020;In press.

Cordell D, White S. Sustainable phosphorus measures: Strategies and technologies for achieving phosphorus security. Argonomy 2013;3:86-116.

Dai L, Wu B, Tan F, He M, Wang W, Qin H, et al. Engineered hydrochar composites for phosphorus removal/recovery: Lanthanum doped hydrochar prepared by hydrothermal carbonization of lanthanum pretreated rice straw. Bioresource Technology 2014;161:327-32.

Desmidt E, Ghyselbrecht K, Zhang Y, Pinoy L, Van der Bruggen B, Verstraete W, et al. Global phosphorus scarcity and full-scale P-recovery techniques: A review. Critical Reviews in Environmental Science and Technology 2015;45:336-84.

European Commission. Study on the Review of the List of Critical Raw Materials: Criticality Assessments. Luxembourg: Publications Office of the European Union; 2017.

European Commission. Study on the EU's List of Critical Raw Materials (2020): Final Report. Luxembourg: Publications Office of the European Union; 2020.

Fang J, Gao B, Chen J, Zimmerman AR. Hydrochars derived from plant biomass under various conditions: Characterization and potential applications and impacts. Chemical Engineering Journal 2015;267:253-9.

Fang C, Zhang T, Li P, Jiang R-F, Wang Y-C. Application of magnesium modified corn biochar for phosphorus removal and recovery from swine wastewater. International Journal of Environmental Research and Public Health 2014; 11(9):9217-37.

Guo S, Dong X, Wu T, Shi F, Zhu C. Characteristic evolution of hydrochar from hydrothermal carbonization of corn stalk. Journal of Analytical and Applied Pyrolysis 2015;116:1-9.

He H, Zhang N, Chen N, Lei Z, Shimizu K, Zhang Z. Efficient phosphate removal from wastewater by MgAl-LDHs modified hydrochar derived from tobacco stalk. Bioresource Technology Reports 2019;8:100348.

Hoekman SK, Broch A, Robbins C. Hydrothermal carbonization (HTC) of lignocellulosic biomass. Energy Fuels 2011; 25(4):1802-10.

Hotová G, Slovák V, Zelenka T, Maršálek R, Parchaňská A. The role of the oxygen functional groups in adsorption of copper (II) on carbon surface. Science of The Total Environment 2020;711:135436.

Jain A, Balasubramanian R, Srinivasan MP. Hydrothermal conversion of biomass waste to activated carbon with high porosity: A review. Chemical Engineering Journal 2016; 283:789-805.

Jian X, Zhuang X, Li B, Xu X, Wei Z, Song Y, et al. Comparison of characterization and adsorption of biochars produced from hydrothermal carbonization and pyrolysis. Environmental Technology and Innovation 2018;10:27-35.

Kosmulski M. Isoelectric points and points of zero charge of metal (hydr)oxides: 50 years after Parks' review. Advances in Colloid and Interface Science 2016;238:1-61.

Kundu S, Coumar MV, Rajendiran S, Kumar A, Rao AS. Phosphates from detergents and eutrophication of surface water ecosystem in India. Current Science 2015;108(7),1320-5.

Mahmoud ZH. The magnetic properties of alpha phase for iron oxide NPs that prepared from its salt by novel photolysis method. Journal of Chemical and Pharmaceutical Research 2017;9(8):29-33.

Martinez-Hernandez E, Amezcua-Allieri MA, Sadhukhan J, Anell JA. Sugarcane bagasse valorization strategies for bioethanol and energy production. In: de Oliveira AB, editor. Sugarcane-Technology and Research. London, UK: IntechOpen; 2018. p. 71-83.

Mokhena TC, Mochane MJ, Motaung TE, Linganiso LZ, Thekisoe OM, Songca SP. Sugarcane bagasse and cellulose polymer composites. In: de Oliveira AB, editor. Sugarcane-Technology and Research. London, UK: IntechOpen; 2018. p. 225-40.

Murray CJ, Müller-Karulis B, Carstensen J, Conley DJ, Gustafsson BG, Andersen JH. Past, present and future eutrophication status of the Baltic Sea. Frontiers in Marine Science 2019;6:No.2.

Nguyen DH, Tran HN, Chao H-P, Lin C-C. Effect of nitric acid oxidation on the surface of hydrochars to sorb methylene blue: An adsorption mechanism comparison. Adsorption Science and Technology 2019;37(7-8):607-22.

Niinipuu M, Latham KG, Boily J-F, Bergknut M, Jansson S. The impact of hydrothermal carbonization on the surface functionalities of wet waste materials for water treatment applications. Environmental Science and Pollution Research 2020;27(19):24369-79.

Nunes CA, Guerreiro MC. Estimation of surface area and pore volume of activated carbons by methylene blue and iodine numbers. Química Nova 2011;34(3):472-6.

Qin C, Liu H, Liu L, Smith S, Sedlak DL, Gu AZ. Bioavailability and characterization of dissolved organic nitrogen and dissolved organic phosphorus in wastewater effluents. Science of the Total Environment 2015;511:47-53.

Petrović JT, Stojanović MD, Milojković JV, Petrović MS, Šoštarić TD, Laušević MD, et al. Alkali modified hydrochar of grape pomace as a perspective adsorbent of Pb^{2+} from aqueous solution. Journal of Environmental Management 2016; 182:292-300.

Sun K, Ro K, Guo M, Novak J, Mashayekhi H, Xing B. Sorption of bisphenol A, 17α-ethinyl estradiol and phenanthrene on thermally and hydrothermally produced biochars. Bioresource Technology 2011;102(10):5757-63.

Tang Q, Shi C, Shi W, Huang X, Ye Y, Jiang W, et al. Preferable phosphate removal by nano-La(III) hydroxides modified mesoporous rice husk biochars: Role of the host pore structure and point of zero charge. Science of the Total Environment 2019;662:511-20.

Tarayre C, De Clercq L, Charlier R, Michels E, Meers E, Camargo-Valero M, et al. New perspectives for the design of sustainable bioprocesses for phosphorus recovery from waste. Bioresource Technology 2016;206:264-74.

Thawornchaisit U, Donnok K, Samphoanoi N, Pholsil P. Iron-modified biochar derived from rice straw for aqueous phosphate removal. Current Applied Science and Technology 2019;19(3):263-75.

United States Department of Agriculture (USDA). Adding value to sugar crop trash and byproduct [Internet]. 2018 [cited 2021 Feb 4]. Available from: https://agresearchmag.ars.usda.gov/2018/feb/sugar.

United States Geological Survey (USGS). Phosphate rock [Internet]. 2021 [cited 2021 May 25]. Available from: https://pubs.usgs.gov/periodicals/mcs2021/mcs2021-phosphate.pdf.

Wang T, Zhai Y, Zhu Y, Peng C, Xu B, Wang T, et al. Acetic acid and sodium hydroxide-aided hydrothermal carbonization of woody biomass for enhanced pelletization and fuel properties. Energy Fuels 2017;31(11):12200-8.

Xiao L-P, Shi Z-J, Xu F, Sun R-C. Hydrothermal carbonization of lignocellulosic biomass. Bioresource Technology 2012; 118:619-23.

Yang Q, Wang X, Luo W, Sun J, Xu Q, Chen F, et al. Effectiveness and mechanisms of phosphate adsorption on iron-modified biochars derived from waste activated sludge. Bioresource Technology 2018;247:537-44.

Yu Y, Yang X, Lei Z, Yu R, Shimizu K, Chen N, et al. Effects of three microelement cations on P mobility and speciation in sewage sludge derived hydrochar by using hydrothermal treatment. Bioresource Technology Reports 2019;7:100231.